SINGLE-PHASE TRANSFORMER LESS SINGLE-STAGE GRID-CONNECTED PV SYSTEM

K. Anil Kumar Reddy[1], P. Surajith Reddy[2]

[1] *M.Tech Student, Dept. of Electrical Engg, JNTUA College of Engineering, Anantapuramu, India-515002*
[2] *M.Tech Student, Dept. of Electrical Engg, JNTUA College of Engineering, Anantapuramu, India-515002*

---***---

Abstract - ***In this article, a single-phase, single-stage current source inverter-based photovoltaic system for grid connection is proposed. Without need of a transformer this system uses the conversion in one step for monitoring the maximum power point and for interfacing photovoltaic system to grid and maximum power point was tracked by the fuzzy logic controller. To control the current injected into the network a proportional resonant-controller is used. To improve the efficiency and power quality of the system a double tuned parallel resonant network is used for reducing the second order and fourth order harmonics at the inverter dc side. A modified carrier based modulation technique is proposed to the current source inverter for magnetize the DC link inductor and by shorting one of bridge converter legs after every active switching cycle. Simulation results validate dynamic performance and the power quality of a proposed system.***

Index Terms- Current source inverter (CSI), grid-connected, maximum power point tracking (MPPT), photovoltaic (PV).

I. INTRODUCTION

Due to the environmental issues, renewable energy source is the main thing in researchers. The most important renewable energy is a photovoltaic (PV) system, because of suitable in distributed generation, satellite system and transportation.

In distributed generation applications, the PV system operated in grid connected mode is very popular. In this grid connected mode, maximum power is from the PV system to supply into the grid. A two stage grid connected PV system utilizes two conversion stages: a dc/dc converter for Boosting and conditioning the PV output voltage and tracking the MPP, and dc/ac inverter for interfacing the PV system to the grid.

In this method, high-voltage PV array is not required, because of dc voltage boosting stage. This two stages suffers from reduced efficiency, higher cost and larger size. The conventional voltage source inverter (VSI) is the most commonly used in grid connected PV system. However, the voltage buck properties of the VSI increase the necessity of using bulky transformer or high dc voltage .However, the electrolytic capacitor, which presents a critical point of failure. The three phase grid connected CSI, which affect the MPPT, reduce the PV life time and associated with odd order harmonics. Therefore, eliminating the harmonics on the dc side various techniques have been proposed to reduce the harmonics CSI PV applications.

The Nonlinear Pulse Width Modulation (NPWM) has been proposed to improve the harmonics mitigation. The power oscillating effect is mitigated by using carrier signal on Pulse Width Modulation (PWM). These techniques not suited in single stage grid connected system because of dc current oscillation is large, which reduces the system loss and PV life time.

In a single stage connected system, the PV system consists of single conversion unit (dc/ac inverter) to track the maximum power point (MPPT) and interface the PV system to the grid. In this paper CSI has been proposed, because dc input current is continuous and CSI voltage boosting capacity allows a low-voltage PV array to the grid interface without need of a transformer or an additional boosting stage. A double tuned resonant is used to mitigate the harmonics at the dc side. The control structure consists of MPPT, and current loop and voltage loop. The effectiveness and robustness of the proposed system, simulation and practical implemented.

II. SYSTEM DESCRIPTION

A grid connected PV system consists of Single-phase Single-stage CSI is shown in FIG.1. This inverter has four Insulated Gate Bipolar Transistors (IGBT) and four diodes. Each diode is connected in series with IGBTs switch for reverse blocking capability. A double tuned parallel resonant filter is series with dc link inductor for smoothing dc link current. A C-L filter is connected in the ac side because it is used for getting the smooth the edges.

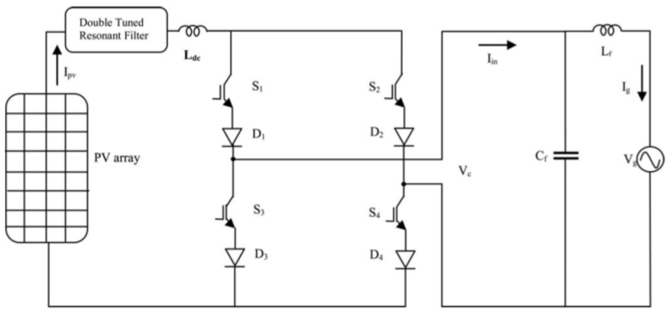

FIG. 1. Single phase grid connected CSI.

III. BLOCK DIAGRAM

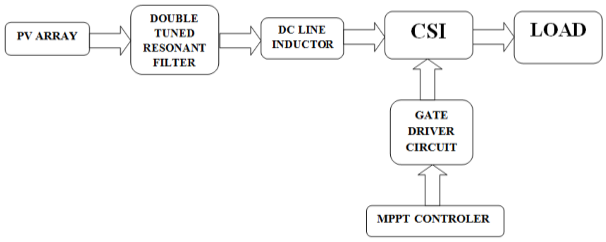

Our aim is synchronize the PV array and the grid. The PV array produces the dc voltage depends upon the irradiation and ambient temperature. This dc voltage flows through the double tuned parallel resonant filter and dc link inductor.

IV. DOUBLE TUNED RESONANT FILTER

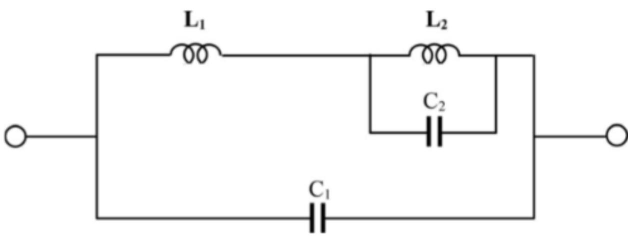

FIG. 2. Proposed double-tuned resonant filter.

In single phase CSI, pulsating power of system frequency generates even harmonics in dc link current. These harmonics reflect on the ac side of voltage and current. These harmonics affect the MPPT in PV system applications and reduce the PV lifetime. Therefore mitigate the harmonics both ac and dc side, the large size dc link inductance to enough the suppress dc link current ripple harmonics. Practically large size dc link inductance not acceptable because of size and cost. To reduce the dc link inductance, parallel resonant filter is used. This filter is capable of smoothing dc link current by using small inductance.

The current source inverter has become a preferred topology for interfacing PV system to the ac power grid, because of CSI provides a continuous dc side current, which is important for PV applications. The energy storing element of CSI has a longer lifetime than VSI. The CSI voltage boosting capacity allows a low voltage PV array to the grid interface without need of transformer or additional boosting stage.

The MPPT get signals from PV array and output (from ac side) of the system. Manipulates the signal and gives out PWM signal to on and off the CSI. So this switching is converted DC to AC pulses and ready for grid synchronization. The oscillating power effect from the grid network is reduced by employing a tuned proportional resonant controller.

To adjust the filter resonance to the desired harmonic frequencies, C_1 impedance and total impedance of L_1, L_2, C_2 and must have equal values of opposite sign. For simplicity, suppose component resistances are small, and can therefore be neglected in the calculation.

$$Z_{c1} + Z_t = 0 \quad (1)$$

From (1), the capacitances C_1 and C_2 are represented by the following equations:

$$C_1 = \frac{L_2 C_2 - \frac{1}{\omega^2}}{\omega^2 L_1 L_2 C_2 - L_1 - L_2} \quad (2)$$

$$C_2 = \frac{-L_2}{\frac{L_2}{C_1} - \omega^2 L_1 L_2} + \frac{1}{\omega^2 L_2} \quad (3)$$

Where C_1 and C_2 are the resonant filter capacitances, L_1 and L_2 are the resonant filter inductances, Z_{C1} is C_1 impedance, Z_t is the total impedance of L_1, L_2, and C_2, and ω is the angular frequency of the second- or fourth-orders harmonics, as shown in fig. 2.

V. MODIFIED CARRIER BASED PWM

Modified carrier based PWM is proposed to control the switching pattern for the single phase grid connected CSI. To provide a continuous path for the dc side current, at least one top switch in either arm and one bottom switch must be turned on during every switching period. In this fig. 4 shows reference and carrier waveform along with switching patterns. The carrier wave with solid line the straight for upper switches while dashed line is lower switches and shifted by 180°. The switching action of each IGBT is equally distributed during every fundamental period.For understanding the switching patterns of the above proposed CPWM, Fig.3. is divided in 10 regions (t_1 – t_{10}), and this each region represents one carrier period frequency. This table shows the switching combinations for that each 10 regions.

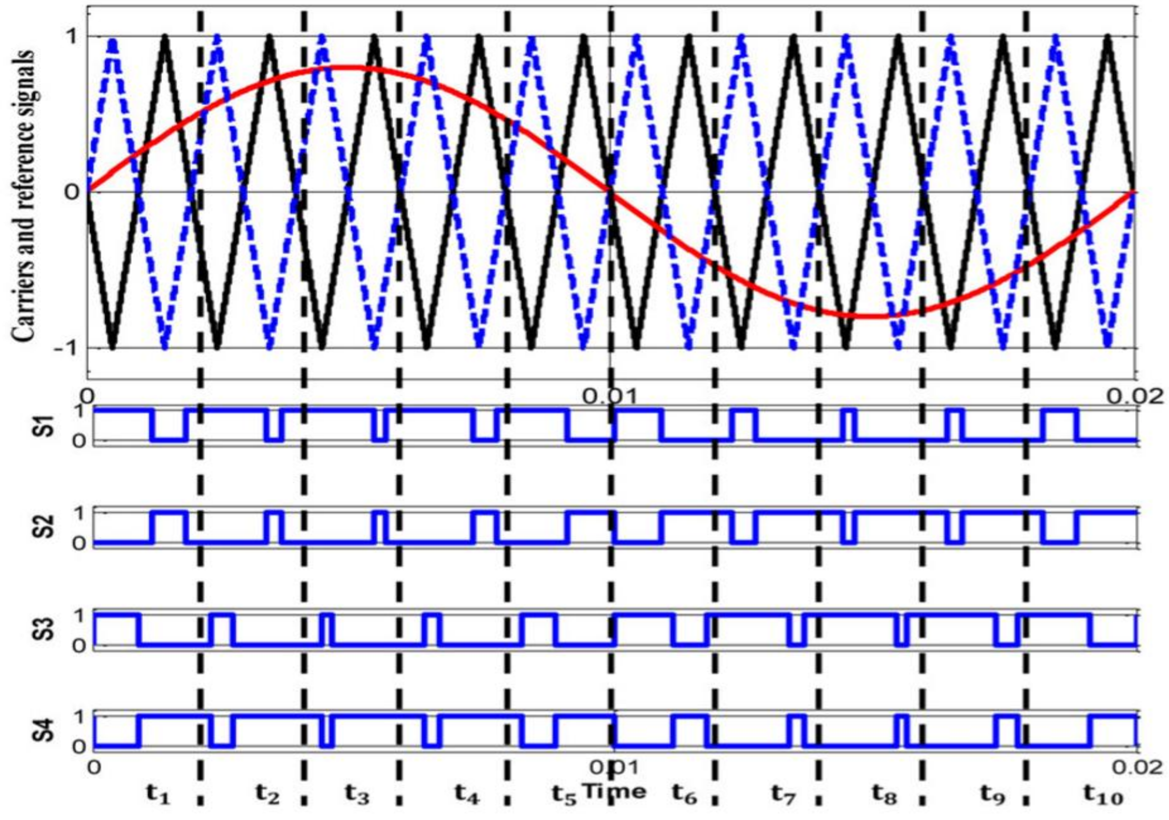

Fig.3. Proposed carriers- based PWM along with switching sequence for one fundamental frequency.

TABLE I
SWITCHING COMBINATION SEQUENCE

Region	Combination sequence
t_1	$(s_1\text{-}s_3)(s_1\text{-}s_4)(s_2\text{-}s_4)(s_1\text{-}s_4)$
t_2	$(s_1\text{-}s_3)(s_1\text{-}s_4)(s_2\text{-}s_4)(s_1\text{-}s_4)$
t_3	$(s_1\text{-}s_3)(s_1\text{-}s_4)(s_2\text{-}s_4)(s_1\text{-}s_4)$
t_4	$(s_1\text{-}s_3)(s_1\text{-}s_4)(s_2\text{-}s_4)(s_1\text{-}s_4)$
t_5	$(s_1\text{-}s_3)(s_1\text{-}s_4)(s_2\text{-}s_4)$
t_6	$(s_1\text{-}s_3)(s_2\text{-}s_3)(s_2\text{-}s_4)(s_2\text{-}s_3)$
t_7	$(s_1\text{-}s_3)(s_2\text{-}s_3)(s_2\text{-}s_4)(s_2\text{-}s_3)$
t_8	$(s_1\text{-}s_3)(s_2\text{-}s_3)(s_2\text{-}s_4)(s_2\text{-}s_3)$
t_9	$(s_1\text{-}s_3)(s_2\text{-}s_3)(s_2\text{-}s_4)(s_2\text{-}s_3)$
t_{10}	$(s_1\text{-}s_3)(s_2\text{-}s_3)(s_2\text{-}s_4)$

VI. PROPOSED SYSTEM

To design a grid connected PV system using CSI, the relationship between the PV output voltage and grid voltage. PV output power is equal to the grid power. PV output voltage should not exceed half the grid peak voltage. The CSI is utilized to track the PV MPP and to interface the PV system to the grid.

Here we are using incremental conductance method to track MPP. In incremental conductance method the array terminal voltage is always adjusted according to the MPP voltage it is based on the incremental and instantaneous conductance of the PV module.

Fig-4 shows that the slope of the P-V array power curve is zero at The MPP, increasing on the left of the MPP and decreasing on the Right hand side of the MPP. The basic equations of this method are as follows.

$dI/dV = -I/V$ At MPP

$dI/dV > -I/V$ Left of MPP

$dI/dV < -I/V$ Right of MPP

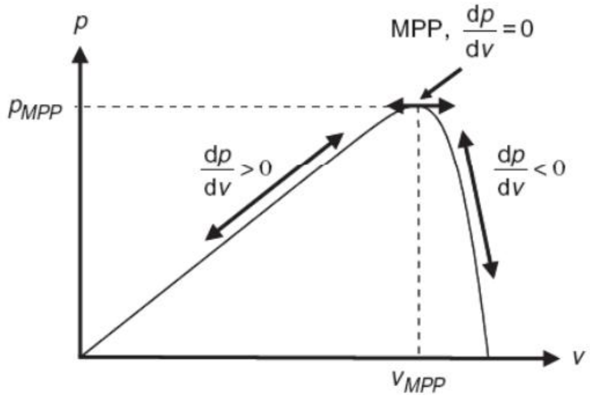

Fig. 4. Basic idea of incremental conductance method on a P-V Curve of solar module

Where I and V are P-V array output current and voltage respectively. The left hand side of equations represents incremental conductance of P-V module and the right hand side represents the instantaneous conductance. When the ratio of change in output conductance is equal to the negative output conductance, the solar array will operate at the maximum power point.

For precise control of the given single-phase inverter, proportional resonant (PR) controller is employed in the voltage loop and current loop controllers. The basic principle of the PR controller is to introduce an infinite gain at selected resonant frequency in order to eliminate steady-state error at that frequency. The PR controller transfer function is given as

$$y = K_p e + K_i \frac{es}{s^2 + \omega_0^2} \quad (4)$$

Where K_p is the proportional gain, K_i is the integral gain, e is the signal error, and ω_o is the fundamental angular frequency.

Let

$$z(s) = K_i \frac{s}{s^2 + \omega_0^2} e(s) \quad (5)$$

Rearrange (5) as

$$sz(s) + \frac{\omega_0^2}{s} z(s) = K_i e(s) \quad (6)$$

Let .

$$\omega(s) = \frac{\omega_0^2}{s} z(s) \quad (7)$$

By taking the derivative of (6) and (7) we have

$$\frac{d\omega(t)}{dt} = \omega_0^2 z(t) \quad (8)$$

$$\frac{dz(t)}{dt} = K_i e - \omega(t) \quad (9)$$

From (4), (8), and (9), the output of the PR controller can be rewritten as

$$y = K_p e(t) + z(t) \quad (10)$$

Table II

DESIGN SPECIFICATIONS AND CIRCUIT PARAMETERS

Item	Value
PV open circuit voltage, V_{oc}(V)	80
PV short circuit current, I_{sc}(A)	15
PV array rated power, P_R(W)	500
Resonant filter inductor, L_1(mH)	10
Resonant filter inductor, L_2(mH)	5
Resonant filter Capacitor, C_1(μF)	125
Resonant filter Capacitor, C_2(μF)	250
Dc link inductor, L_{dc}(mH)	5
Switching frequency, f_s(kHz)	4
AC line inductor, (mF)	1
AC line capacitor, C(μF)	20
Grid voltage, $V_{g,rms}$(V)	110

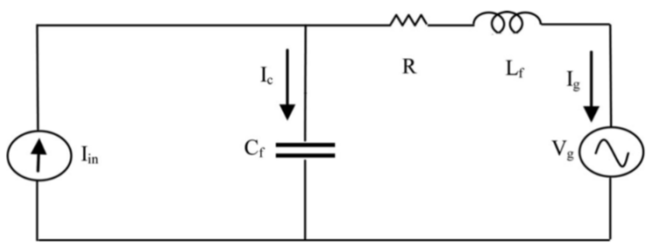

Fig. 5. Equivalent circuit of the CSI ac side

From the equivalent circuit of the CSI ac side, which is shown in Fig. 5 and the PR controller equations, the ac current and voltage loops are designed, where I_{in} is the CSI output current, C_f is the filter capacitor, L_f is the filter inductor, R is the inductor internal resistor, I_c is the current passing through the capacitor, I_g is the grid current, and V_g is the grid voltage.

The differential equation that describes the ac-side dynamic voltage is

$$\frac{dI_g}{dt} = \frac{-R}{L} I_g + \frac{V_c - V_g}{L} \quad (11)$$

Let

$$u = v_c - v_g \quad (12)$$

From (11) and (12), by feeding the grid current error to the PR controller, the value of u is obtained from (10) as

$$u(t) = k_{pi}\left(I_{g,ref}(t) - I_g(t)\right) + z_i(t) \quad (13)$$

Substituting (13) into (11)

$$\frac{di_g}{dt} = \frac{1}{L}(k_{pi} I_{g,ref}(t) - k_{pi} I_g(t) - R I_g(t) + Zi(t) \quad (14)$$

Where

$$\frac{dz_i(t)}{dt} + \omega_0{}^2 \int z_i(t)dt = k_{ii}\left(I_{g,ref}(t) - I_g(t)\right) \quad (15)$$

and

$$\omega_i(t) = \int \omega_0{}^2 z_i(t)dt \quad (16)$$

Where k_{pi} is the current controller proportional gain and k_{ii} is the current controller integral gain.

By taking the derivative of (15) and (16)

$$\frac{dz_i(t)}{dt} = k_i\left(I_{g,ref}(t) - I_g(t)\right) - \omega_i(t) \quad (17)$$

$$\frac{d\omega_i(t)}{dt} = \omega_0{}^2 z_i(t) \quad (18)$$

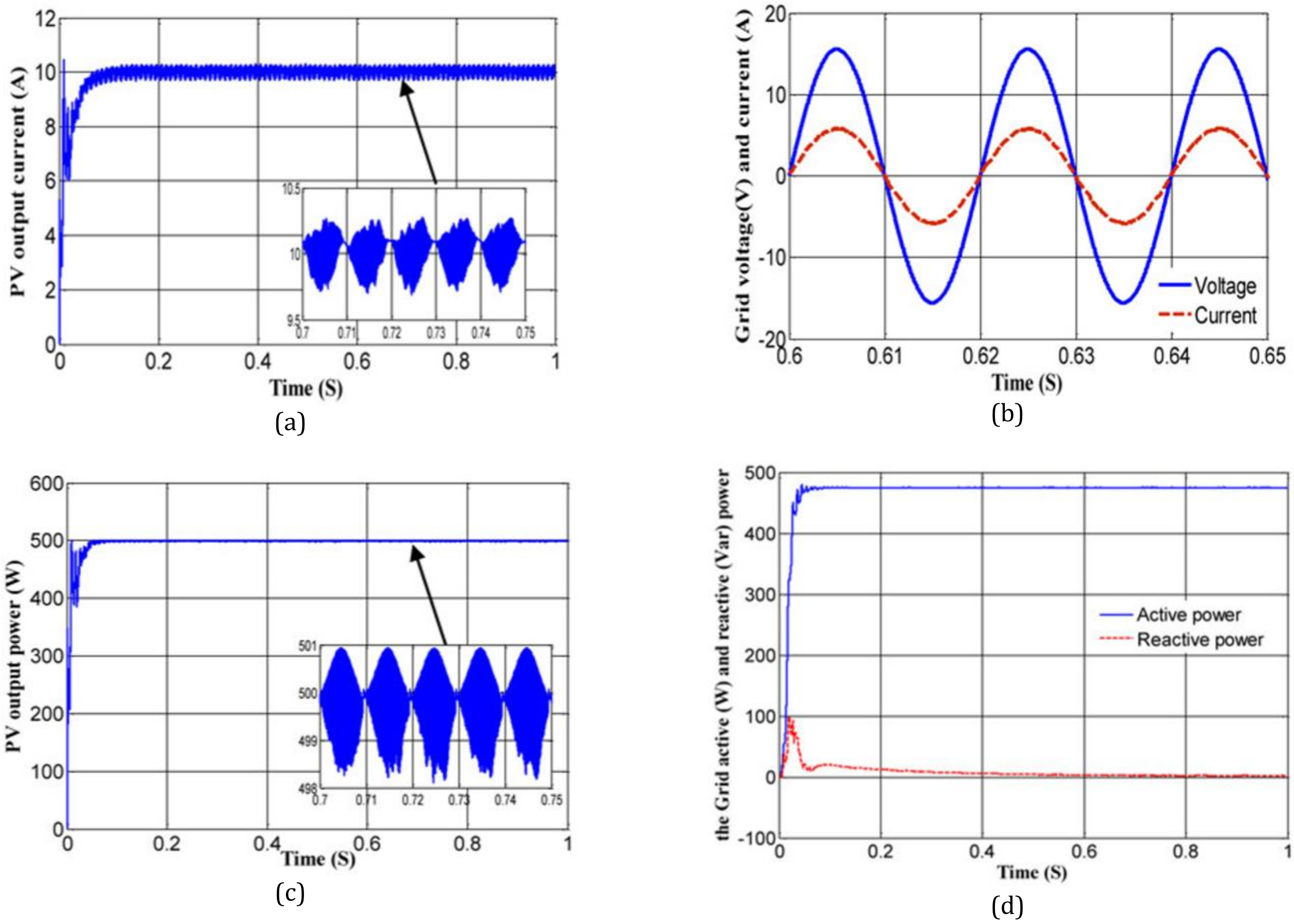

Fig. 6. (a) PV output current, (b) grid voltage (factored by 10) and current, (c) PV output power, and (d) grid active and reactive power.

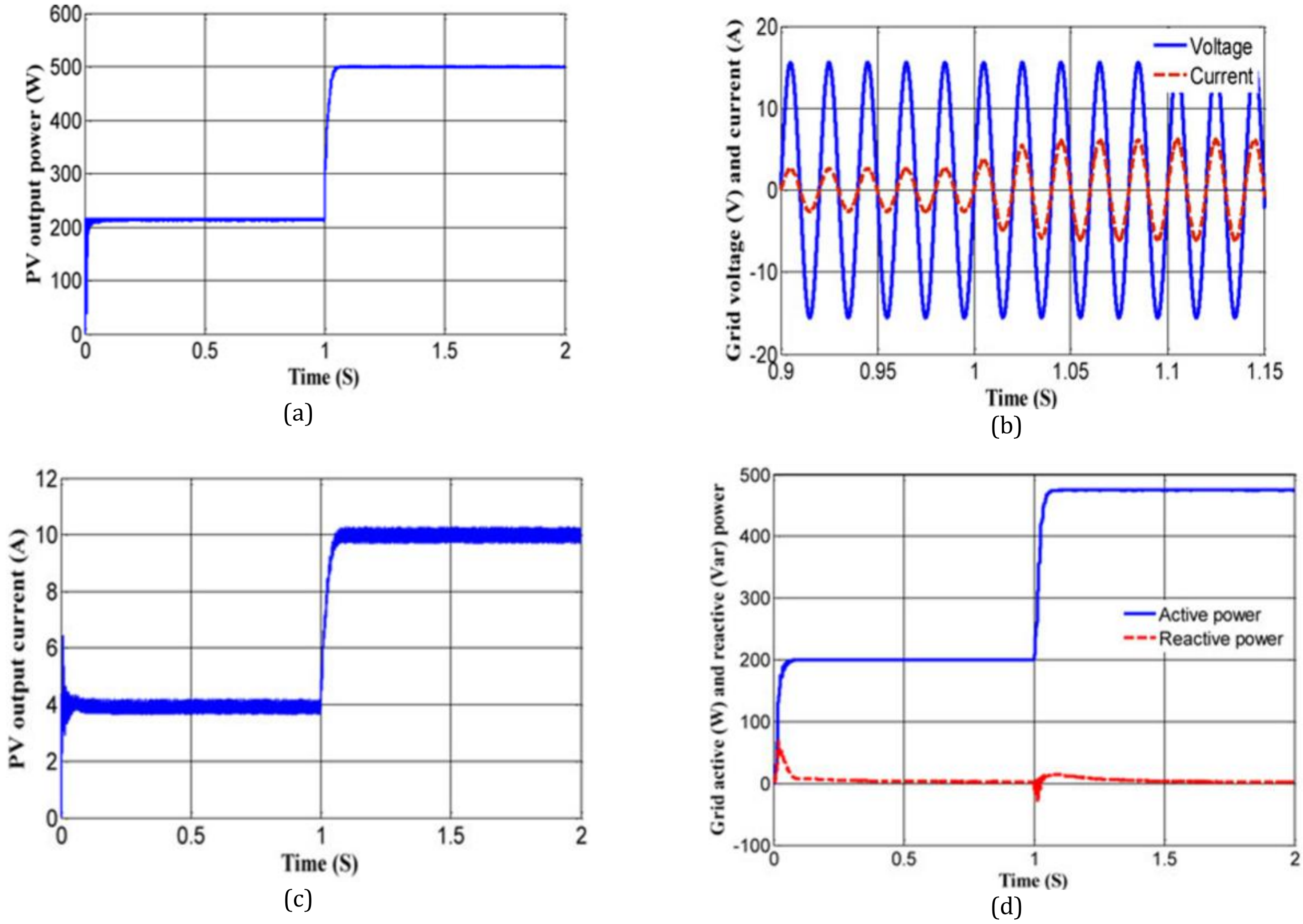

Fig. 7. Simulation results of the proposed system under two radiation levels: 500 and 1000 W/m2. (a) PV output power, (b) grid voltage (factored by 10) and current (c) PV output current, and (d) grid active and reactive power.

From (14), (17), and (18), the state- space model of the current-loop controller is obtained as

$$\frac{d}{dt}\begin{pmatrix} I_g(t) \\ z_i(t) \\ \omega_i(t) \end{pmatrix} = \begin{pmatrix} \frac{-R+K_{ii}}{L} & \frac{1}{L} & 0 \\ -K_{ii} & 0 & -1 \\ 0 & \omega_0^2 & 0 \end{pmatrix} \begin{pmatrix} I_g(t) \\ z_g(t) \\ \omega_i(t) \end{pmatrix} + \begin{pmatrix} \frac{K_{pi}}{L} \\ K_{ii} \\ 0 \end{pmatrix} I_{g,ref}\ (t) \tag{19}$$

Similarly, the state-space model of the voltage loop controller is

$$\frac{d}{dt}\begin{pmatrix} V_c(t) \\ z_v(t) \\ \omega_v(t) \end{pmatrix} = \begin{pmatrix} \frac{-K_{pv}}{C} & \frac{1}{C} & 0 \\ -K_{ic} & 0 & -1 \\ 0 & \omega_0^2 & 0 \end{pmatrix} \begin{pmatrix} V_c(t) \\ z_v(t) \\ \omega_v(t) \end{pmatrix} + \begin{pmatrix} \frac{K_{pv}}{L} \\ K_{ic} \\ 0 \end{pmatrix} V_{g,ref}\ (t) \tag{20}$$

To obtain the overall state-space model of the controllers is rewritten as

$$\frac{d}{dt}\begin{pmatrix} V_c(t) \\ z_v(t) \\ \omega_v(t) \\ I_g(t) \\ z_i(t) \\ \omega_i(t) \end{pmatrix} = \begin{pmatrix} \frac{-k_{pv}}{c} & \frac{1}{c} & 0 & \frac{k_{pv}k_{pi}}{c} & \frac{k_{pv}}{c} & 0 \\ -k_{iv} & 0 & -1 & k_{iv}k_{pi} & k_{iv} & 0 \\ 0 & \omega_0{}^2 & 0 & 0 & 0 & 0 \\ 0 & 0 & 0 & \frac{-k_{pi}}{L} & \frac{1}{L} & 0 \\ 0 & 0 & 0 & -k_{ii} & 0 & -1 \\ 0 & 0 & 0 & 0 & \omega_0{}^2 & 0 \end{pmatrix} \times \begin{pmatrix} V_c(t) \\ z_v(t) \\ \omega_v(t) \\ I_g(t) \\ z_i(t) \\ \omega_i(t) \end{pmatrix} + \begin{pmatrix} \frac{k_{pv}k_{pi}}{c} & \frac{k_{pv}}{c} \\ k_{iv}k_{pi} & k_{iv} \\ 0 & 0 \\ \frac{k_{pi}}{L} & 0 \\ k_{ii} & 0 \\ 0 & 0 \end{pmatrix} \begin{pmatrix} I_{g,ref}(t) \\ V_g(t) \end{pmatrix} \quad (21)$$

VII. CONCLUSION

A single stage single phase grid connected PV system using CSI has been meet the grid requirements without using high dc voltage or a bulky transformer. The control structure consists of MPPT to improve the system performance during normal and varying weather conditions. A single stage system, PV power is delivered to the grid with high efficiency, low cost. A modified carrier based modulation technique is to provide short circuit path on the dc side. A double tuned resonant filter is proposed to suppress the harmonics with small inductance.

VIII. REFERECE

[1] Y. Bo, L.Wuhua, Z. Yi, and H. Xiangning, "Design and analysis of a gridconnected photovoltaic power system," IEEE Trans. Power Electron.,vol. 25, no. 4, pp. 992–1000, Apr. 2010.

[2] S. B. Kjaer, J. K. Pedersen, and F. Blaabjerg, "A review of single-phasegrid-connected inverters for photovoltaic modules," IEEE Trans. Ind.Appl., vol. 41, no. 5, pp. 1292–1306, Sep.– Oct. 2005

[3] S. Jain and V. Agarwal, "A single-stage grid connected inverter topology for solar PV systems with maximum power point tracking," IEEE Trans. Power Electron., vol. 22, no. 5, pp. 1928– 1940, Sep. 2007.

[4] E. Villanueva, P. Correa, J. Rodriguez, and M.Pacas, "Control of a single phase cascaded H-bridge multilevel inverter for grid-connected photovoltaic systems," IEEE Trans. Ind. Electron., vol. 56, no. 11, pp. 4399–4406, Nov. 2009.

[5] W. Tsai-Fu, C. Chih-Hao, L. Li-Chiun, and K. Chia-Ling, "Power losscomparison of single- and two-stage grid-connected photovoltaic systems," IEEE Trans. Energy Convers., vol. 26, no. 2, pp. 707–715, Jun. 2011